

NASA TECHNICAL NOTE



NASA TN D-5704

C. 1

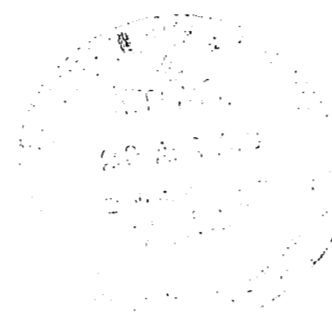
NASA TN D-5704



LOAN COPY: RETURN TO  
AFWL (WLOL)  
KIRTLAND AFB, N MEX

# VAPOR INGESTION PHENOMENON IN HEMISPHERICALLY BOTTOMED TANKS IN NORMAL GRAVITY AND IN WEIGHTLESSNESS

*by Steven G. Berenyi and Kaleel L. Abdalla*  
*Lewis Research Center*  
*Cleveland, Ohio*





0131526

1. Report No. NASA TN D-5704		2. Government Accession No.		3. Recipient's Catalog No.	
4. Title and Subtitle VAPOR INGESTION PHENOMENON IN HEMISPHERICALLY BOTTOMED TANKS IN NORMAL GRAVITY AND IN WEIGHTLESSNESS				5. Report Date April 1970	
				6. Performing Organization Code	
7. Author(s) Steven G. Berenyi and Kaleel L. Abdalla				8. Performing Organization Report No. E-5410	
9. Performing Organization Name and Address Lewis Research Center National Aeronautics and Space Administration Cleveland, Ohio 44135				10. Work Unit No. 124-08	
				11. Contract or Grant No.	
				13. Type of Report and Period Covered Technical Note	
12. Sponsoring Agency Name and Address National Aeronautics and Space Administration Washington, D. C. 20546				14. Sponsoring Agency Code	
15. Supplementary Notes					
16. Abstract An experimental investigation was conducted in normal gravity and in a weightless environment to study the vapor ingestion phenomenon during outflow of liquid from hemispherically bottomed cylinders. The vapor ingestion heights in normal gravity and the critical heights in weightlessness were correlated with Froude and Weber number parameters, respectively. In the normal-gravity correlation, the Froude number parameter was modified by a tank-radius-to-drain-radius ratio. In the weightless tests, the Weber number parameter based on the outflow rate was used. Comparisons with data from flat-bottomed tanks are included, as well as data on liquid residuals at the time of vapor ingestion.					
17. Key Words (Suggested by Author(s)) Weightlessness Vapor ingestion Suction dip Tank draining			18. Distribution Statement Unclassified - unlimited		
19. Security Classif. (of this report) Unclassified		20. Security Classif. (of this page) Unclassified		21. No. of Pages 24	22. Price* \$3.00

\*For sale by the Clearinghouse for Federal Scientific and Technical Information  
Springfield, Virginia 22151

# VAPOR INGESTION PHENOMENON IN HEMISPHERICALLY BOTTOMED TANKS IN NORMAL GRAVITY AND IN WEIGHTLESSNESS

by Steven G. Berenyi and Kaleel L. Abdalla

Lewis Research Center

## SUMMARY

An experimental investigation was conducted in normal gravity and in a weightless environment to study the vapor ingestion phenomenon during outflow of liquid from hemispherically bottomed cylinders. The vapor ingestion heights in normal gravity and the critical heights in weightlessness were correlated with Froude and Weber number parameters, respectively. In the normal-gravity correlation, the Froude number parameter was modified by a tank-radius-to-drain-radius ratio. In the weightless tests, the Weber number parameter based on the outflow rate was used. Comparisons with data from flat-bottomed tanks are included, as well as data on liquid residuals at the time of vapor ingestion.

## INTRODUCTION

The Lewis Research Center has been conducting experimental investigations of the general problem of liquid outflow from tank systems in weightlessness. These studies have examined such areas as interface distortions, vapor ingestion, and liquid residual problems. References 1 and 2 reported observations of the liquid-vapor interface distortions during outflow in weightlessness. It was concluded in these references that the interface distortions were functions of Weber number (the ratio of inertia to surface-tension forces) and initial filling level. In these tests cylindrical tanks with various tank-bottom shapes were used, and the results showed that the distortions observed were independent of these bottom shapes.

The related problem of vapor ingestion has been discussed in some detail in references 3 to 6. References 3 and 4 were normal-gravity simulations of low-gravity outflow in flat-bottomed tanks, and showed correlations of vapor ingestion heights with Froude number. Reference 4 has also developed an analysis for vapor ingestion, while reference 5 modified this theoretical analysis to include the effects of surface tension.

The resulting expression predicted that vapor ingestion in weightlessness is dependent on the Weber number. The experimental study of reference 6, performed in a weightless environment, indeed resulted in an empirical expression correlating the critical liquid height with the Weber number for flat-bottomed cylindrical tanks.

This report presents the results of an experimental study of the vapor ingestion phenomenon for hemispherically bottomed cylindrical tanks in both normal-gravity and weightless environments. Each tank contained a cylindrical drain located on the center-line. Presented are comparisons with the results obtained in reference 6 for flat-bottomed cylinders. Also included are data on liquid residuals. The tests were conducted at the Lewis Research Center's 2.2-Second Zero-Gravity Facility.

## SYMBOLS

$a$	acceleration, $\text{cm}/\text{sec}^2$
$g_0$	acceleration due to gravity, $980 \text{ cm}/\text{sec}^2$
$h_{\text{cr}}$	critical height, cm
$h_i$	initial liquid height, cm
$h_{\text{vi}}$	vapor ingestion height, cm
$Q_0$	outflow rate, $\text{cm}^3/\text{sec}$
$R$	tank radius, cm
$R/r_0$	radius ratio
$r_0$	outlet radius, cm
$t$	time, sec
$V_0$	average outflow velocity (velocity in outlet line), $\text{cm}/\text{sec}$
$V_T$	average liquid velocity in tank, $\text{cm}/\text{sec}$
We	Weber number, $V_0^2 r_0 / \beta$ or $Q_0^2 / \beta R^3$
$\beta$	specific surface tension, $\sigma/\rho$ , $\text{cm}^3/\text{sec}^2$
$\mu$	absolute viscosity, $\text{g}/(\text{cm}\text{-sec})$
$\rho$	density, $\text{g}/\text{cm}^3$
$\sigma$	surface tension, dynes/cm (or $10^{-5} \text{ N}/\text{cm}$ )

## APPARATUS AND PROCEDURE

Detailed descriptions of the 2.2-Second Zero-Gravity Facility and the experiment apparatus and procedure used are given in the appendix. Briefly, the experimental investigation utilized two hemispherically bottomed cylindrical tanks, 2 and 4 centimeters in radius. Each tank was fitted with a cylindrical outlet line equal to one-fifth, one-tenth, or one-twentieth of the respective tank radius. Details of the tank design are also presented in the appendix. A pressurization technique, described in the appendix, was used to produce the desired flow rate. The draining phenomenon was recorded on film for a range of flow rates in both normal gravity and weightlessness.

The liquid chosen for these tests was anhydrous ethanol with the following properties (at 20° C): surface tension,  $\sigma = 22.3$  dynes per centimeter; density,  $\rho = 0.789$  gram per cubic centimeter; viscosity,  $\mu = 1.2 \times 10^{-2}$  gram per centimeter-second. The liquid exhibited a 0° contact angle with the tank surface. To improve the quality of the photographic data, a small amount of dye was added to the test liquid. Addition of this dye has no measurable effect on the liquid properties.

## DESCRIPTION OF VAPOR INGESTION PHENOMENON

During tank draining there exists a time when the center of the liquid-vapor interface is suddenly drawn toward the outlet. At this time, a dip in the liquid-vapor interface forms above the drain and rapidly accelerates toward the outlet, followed quickly by ingestion of vapor into the outlet line. This phenomenon is illustrated for both normal gravity and weightlessness in figure 1. The sketches in the figure indicate the interface shape during draining, while the displacement-time graphs show the corresponding interface height as a function of draining time.

In the cylindrical section during outflow in normal gravity (fig. 1(a)), the interface moves with a constant velocity until the incipience of vapor ingestion. The interface shape away from the drain remains essentially flat, even at the time of vapor ingestion, as shown in the sketch in figure 1. The displacement-time graph shows the rapid acceleration of the interface centerline towards the outlet, and at the same time depicts the liquid-vapor interface height away from the drain. The height of the liquid-vapor interface at the incipience of vapor ingestion (at the time the dip forms) is called the critical height. At the instant the vapor reaches the outlet line, the interface height away from the drain, where the interface is flat, is denoted as the vapor ingestion height.

To define adequately the vapor ingestion phenomenon, knowledge of either the incipience of vapor ingestion (critical height  $h_{cr}$ ) or vapor ingestion height  $h_{vi}$  is

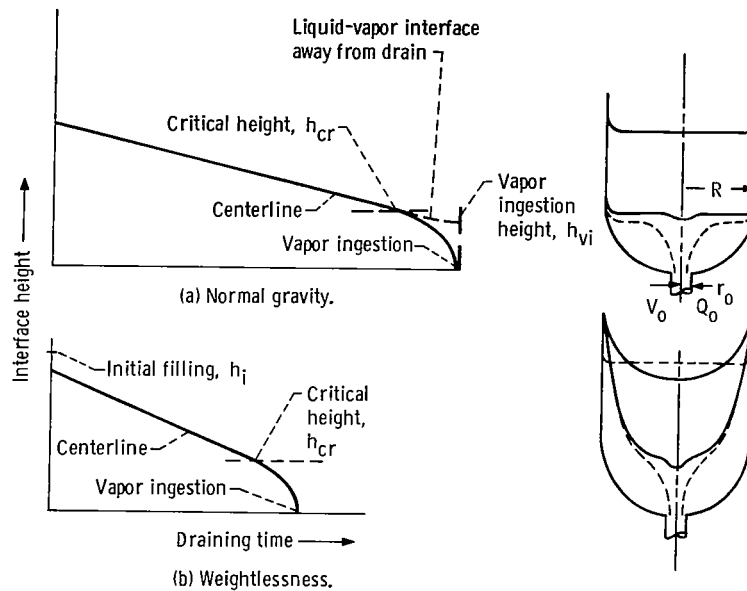
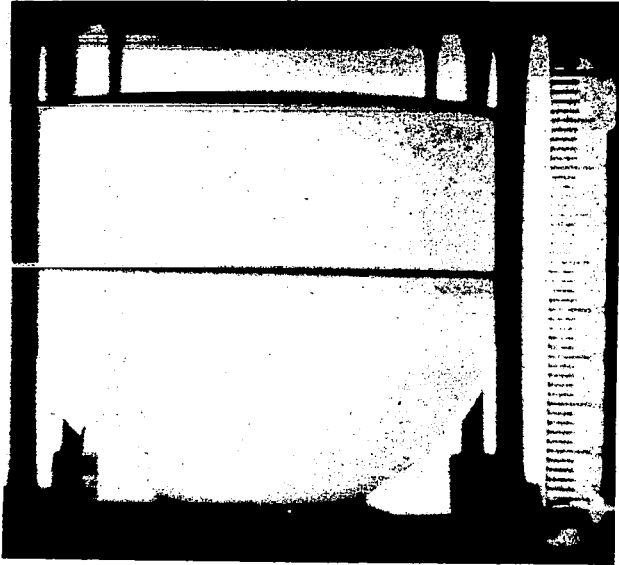


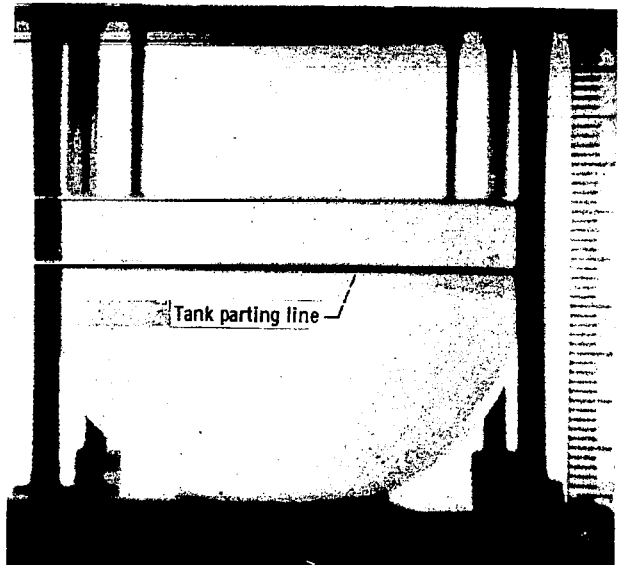
Figure 1 - Vapor ingestion phenomenon.

necessary. The analysis of reference 4 discussed a vapor ingestion height measured away from the drain as a function of Froude number in terms of outflow rate and outlet radius. The analysis was made for a flat-bottomed tank and neglected surface tension. Biliquid experiments were used to verify the analysis. This Froude number criterion seems meaningful for draining in normal gravity, in which (as described earlier) the moving interface does indeed remain flat away from the drain. In describing vapor ingestion in normal gravity, therefore, this vapor ingestion height away from the drain is used.

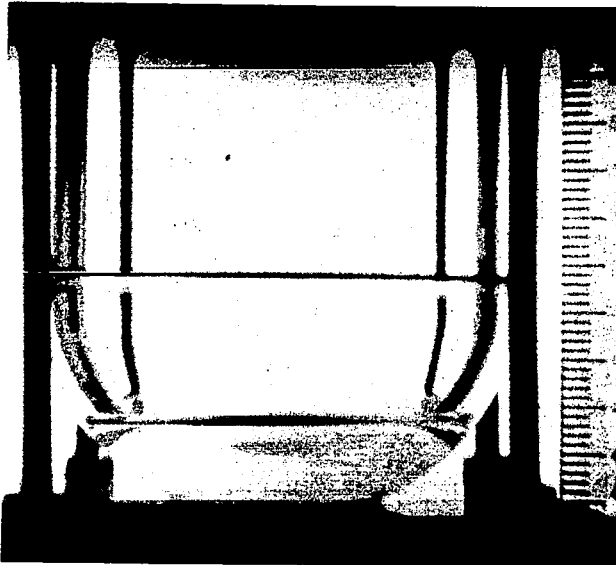
The draining phenomenon in weightlessness has many elements of similarity to that in normal gravity. The shape of the liquid-vapor interface, however, is considerably different, as shown in the sketch of figure 1(b). In weightlessness, the interface prior to draining is a curved surface with a shape determined by liquid-to-solid contact angle. During draining, the interface distorts from this initially curved surface (refs. 1 and 2). As in normal gravity, the interface centerline height moves at nearly a constant velocity until incipience of vapor ingestion and then accelerates into the outlet. Again, the critical height is defined as the liquid-vapor-interface centerline height at the time of incipience of vapor ingestion. For both normal gravity and weightlessness, the critical height occurs at the time when the interface centerline deviates rapidly from constant-velocity draining (see fig. 1). However, in zero gravity, the interface height away from the drain is changing in the radial direction because of the highly curved



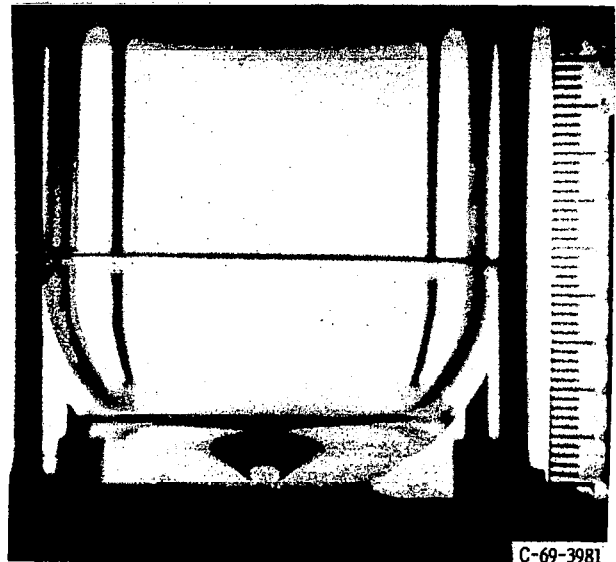
(a-1) Initiation of draining.



(a-2) Interface shape during draining.



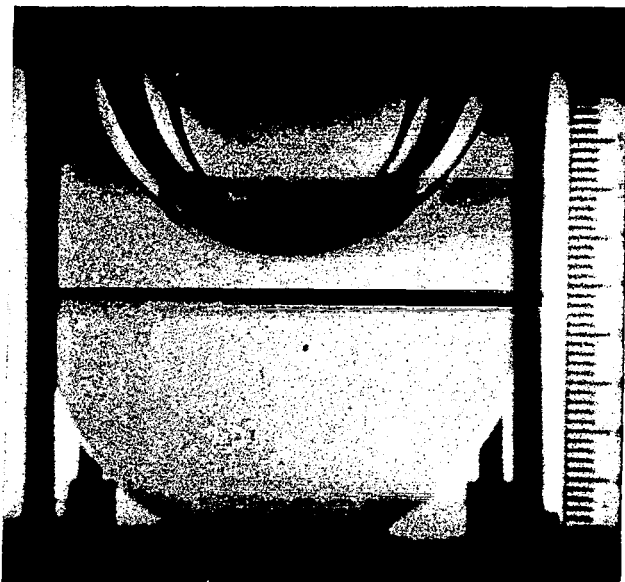
(a-3) Incipience of vapor ingestion.



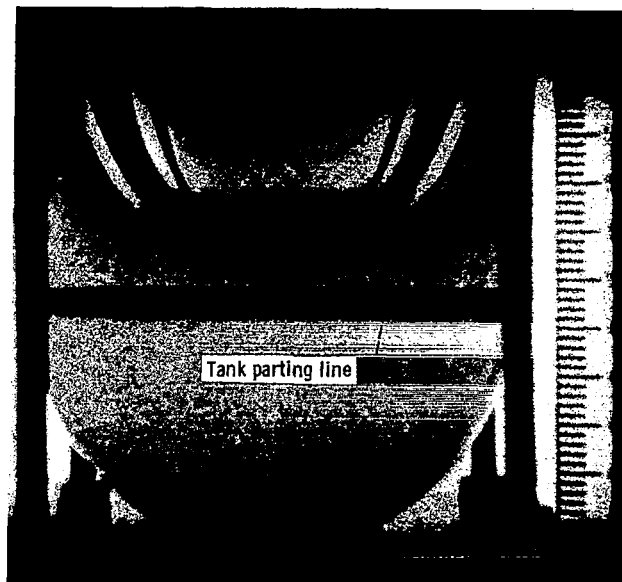
(a-4) Vapor ingestion.

(a) Normal gravity.

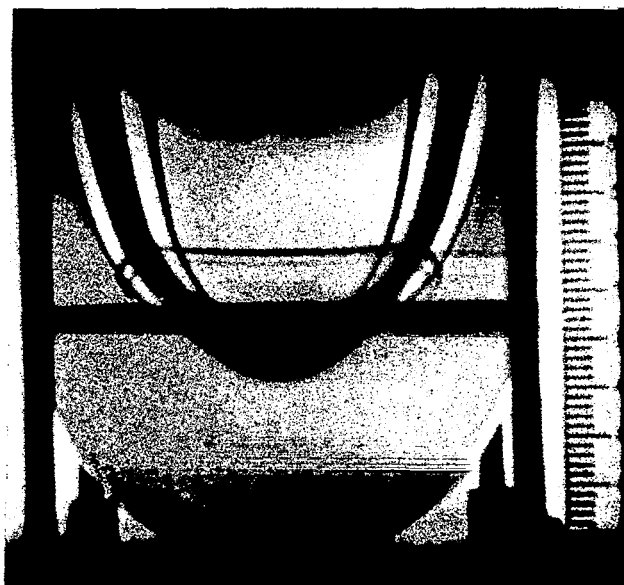
Figure 2. - Vapor ingestion in normal gravity and weightlessness.



(b-1) Initiation of draining.



(b-2) Interface shape during draining.



(b-3) Incipience of vapor ingestion.



(b-4) Vapor ingestion.

(b) Weightlessness.  
Figure 2. - Concluded.

liquid-vapor interface shape. In weightlessness, therefore, the vapor ingestion height is not defined, and the critical height measured directly over the drain has to be used in describing the vapor ingestion phenomenon.

The phenomenon, for both normal gravity and weightlessness, is illustrated in the photographic sequences in figure 2 for typical draining cases. The first photograph in each sequence depicts the initial interface shape. As discussed later, the weightless experiments were performed by allowing sufficient time for the liquid-vapor-interface centerline to reach its low point prior to initiation of draining. This configuration, as shown, is nearly hemispherical in shape (fig. 2(b-1)) compared to the flat interface at normal gravity (fig. 2(a-1)). During draining in normal gravity (fig. 2(a-2)), the interface remains flat, and the liquid residuals are calculated solely from the knowledge of the vapor ingestion height.

However, in weightlessness the already curved interface distorts even more from the initial hemisphere (fig. 2(b-2)). This distortion from the hemisphere causes more liquid to remain on the tank wall, resulting in greater liquid residuals than in the normal-gravity case even at the same critical height. The shapes are also shown at the time the interface reaches the incipience of vapor ingestion (figs. 2(a-3) and (b-3)) and at the instant vapor is ingested in the drain (figs. 2(a-4) and (b-4)).

## RESULTS AND DISCUSSION

### Vapor Ingestion in Normal Gravity

Normal-gravity data were obtained for hemispherically bottomed tanks of 2 and 4 centimeters in radius. Initial liquid fillings of both 2 and 3 tank radii ( $2R$  and  $3R$ ) were used, and the tests included four different outlet-to-tank-radius ratios. For each draining test, a displacement-time curve similar to figure 1(a) was obtained (as described in the appendix). The linear portion of this curve was used to calculate the interface velocity. The average outflow velocity was then computed by the use of the continuity equation for incompressible flow and the known tank-to-outlet-area ratio.

The vapor ingestion height, as defined in the preceding section and depicted on figure 1(a), was determined for each test run and is shown as a function of the outflow velocity in figure 3. Examination of this figure reveals a dependence of vapor ingestion height on both tank and outlet radii, as well as on the outflow velocity. Note that these findings are at variance with those of reference 6, where no effect of tank size was reported. The effects of outflow velocity and outlet size were, however, similar to those obtained in the study of reference 6, which was conducted with flat-bottomed tanks. Also, in those tests (ref. 6) vapor ingestion heights were found to be relatively inde-

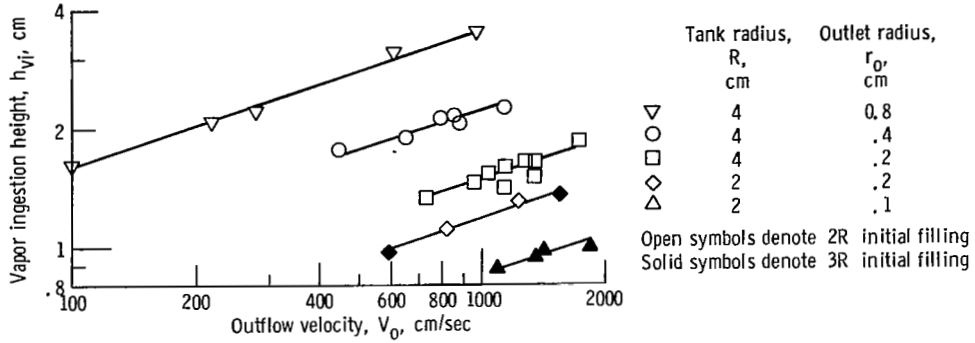


Figure 3. - Vapor ingestion heights in normal gravity.

pendent of initial filling levels. A comparison of 2R and 3R initial fill was made at  $R = 2$  and  $r_o = 0.2$ , and as shown in figure 3 no noticeable effect on the vapor ingestion heights was observed. Therefore, a comprehensive study of the effect of initial fill was not pursued.

Past experimental and theoretical studies with the flat-bottomed tanks (refs. 3, 4, and 6) have effectively demonstrated the correlation of these normal-gravity vapor ingestion heights with some form of a Froude number (the ratio of inertia to gravity forces).

The forms of the Froude correlations used were (from refs. 3 and 4)

$$\frac{h_{vi}}{2R} = 0.43 \tanh \left[ 1.3 \left( \frac{V_T^2}{2ar_o} \right)^{0.29} \right] \quad (1)$$

and

$$\frac{Q_o^2}{gr_o^2 h_{vi}^3} = \frac{6.5}{\left( \frac{r_o}{h_{vi}} \right)^2} \quad (2)$$

where  $g = (\Delta\rho/\rho)g_o$  for their biliquid tests.

A rearranged form of equation (2) using the tank radius for nondimensionalization and given in reference 6 as

$$\frac{Q_o^2}{g_o R^5} = 6.5 \left( \frac{h_{vi}}{R} \right)^5 \quad (3)$$

was used to correlate experimental data of reference 6 for flat-bottomed tanks. In reference 6 the  $g$  was replaced with  $g_o$  for liquid-vapor tests in normal gravity. Appli-

cation of these equations to the present data for hemispherically bottomed tanks resulted in good correlation of the vapor ingestion height with outlet radius but not quite adequate results for the tank radius. To obtain a closer correlation of this data, it is necessary to modify equation (2).

Since the only difference in these normal-gravity tests and those of references 4 and 6 is the tank-bottom geometry, it would seem reasonable to assume that the scaling of the vapor ingestion phenomena could be performed by the use of some similar dynamic scaling parameter (the Froude number) modified by a geometric scaling term to account for the hemispherical bottom. As it was already pointed out, measured vapor ingestion heights in these tests were dependent on both the tank radius and the outlet radius. Because of these observations, the radius ratio  $R/r_o$  was used as the geometric scaling parameter.

Presented in figure 4 are the results of these tests in a form where a nondimensional vapor ingestion height is plotted as a function of a Froude number times a radius ratio squared. The exponent on the radius ratio was determined by the use of curve-fitting techniques. Figure 4(a) depicts a correlation using the Froude number based on outflow rate (ref. 4).

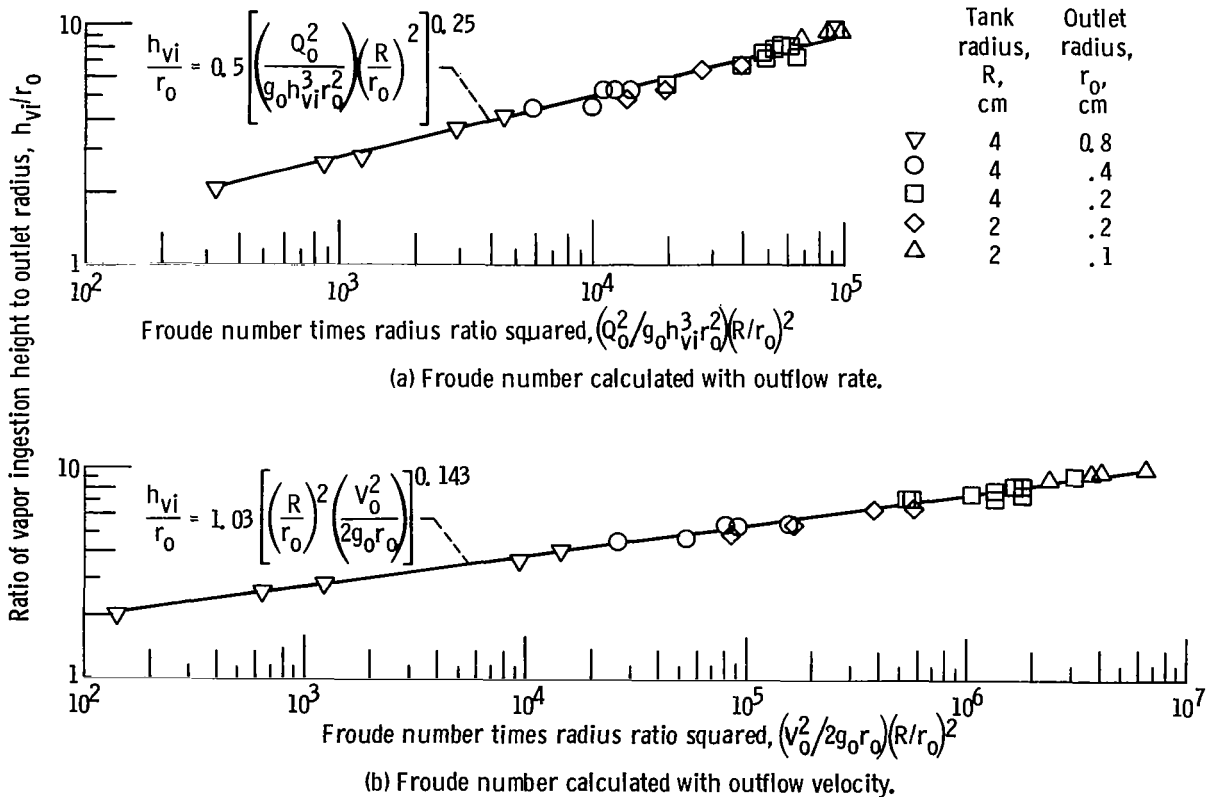


Figure 4. - Vapor ingestion heights in normal gravity correlated with Froude number.

The appearance of the  $h_{vi}$  term on both sides of the correlating equation of this figure makes it inconvenient for use in engineering calculations. It is presented here in this manner only for comparison with the works of others (ref. 4) who have previously used this form of the Froude number. Perhaps a more convenient form may be obtained by plotting the data in a way that separates the dependent variable  $h_{vi}$  from the independent variables. The variables are separated by simple algebraic operations and presented in this new format in figure 4(b). This figure illustrates an approach where the Froude number is calculated based on outlet velocity (similar to ref. 3). The equation of the line shown in figure 4(b) is

$$\frac{h_{vi}}{r_o} = 1.03 \left[ \left( \frac{R}{r_o} \right)^2 \left( \frac{V_o^2}{2g_o r_o} \right) \right]^{0.143} \quad (4)$$

The experimental data points are in excellent agreement with this empirical equation for the 5-decade range of the independent variables for which these data were obtained. In this method of presentation, the Froude number appears in a form that is consistently based on conditions measured at the outlet (in contrast with eq. (1)). Note, however, that each method of presentation indicates the same basic concept, that is, the nondimensional vapor ingestion height is a function of a Froude number times a radius ratio squared. Both forms of the equation of figure 4 contain a dynamic scaling term (Froude number) and a geometric scaling term (the radius ratio). It may also be worthy to note that, unlike the earlier correlations, the empirical correlation of figure 4 is not limited to the case of  $r_o/h_{vi} \ll 1.0$ . The data ranged from  $r_o/h_{vi} = 0.1$  to 0.5. In comparing the data of these present normal-gravity studies with those of reference 6, it was found that for the ranges of flow rates investigated the vapor ingestion heights in the hemispherically bottomed tanks were approximately 10 percent higher than those in the flat-bottomed tanks.

### Vapor Ingestion in Weightlessness

Experimental data were obtained in weightlessness for a range of variables similar to those in normal gravity. The procedures used in obtaining these data were, however, slightly different. When a partly filled cylindrical container is exposed to a weightless environment, the liquid-vapor interface exhibits a damped harmonic oscillation about its static hemispherical equilibrium shape for a short time period. In conducting these tests, a sufficient time was allowed, after placing the system in weightlessness, for the

interface to reach its lowest point in its first oscillation, at which time outflow was initiated (see appendix). The velocity of the center point of the curved interface at this time is zero.

A typical time-displacement history of the motion of this center point after the initiation of draining is illustrated in figure 1(b). As in normal gravity, this interface center point moves at a constant velocity followed by acceleration toward the outlet. The critical height  $h_{cr}$  where the rapid acceleration occurs is denoted in figure 1(b). This critical height was measured and recorded for each weightless test and is presented in figure 5 as a function of outflow velocity. Both the 2R and 3R initial filling data are included in this figure because in previous tests (ref. 6) initial filling level had very little, if any, effect on critical heights.

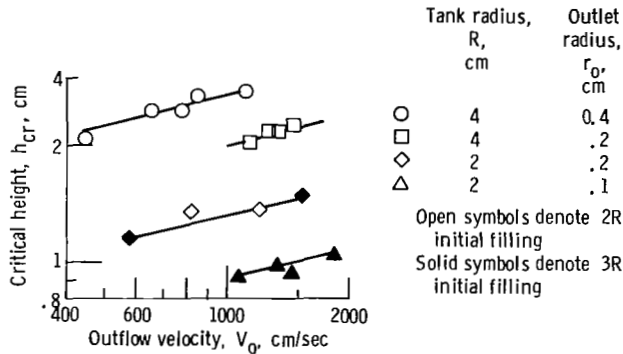


Figure 5. - Critical heights in weightlessness.

The data show an increase in critical height with increasing draining rate; however, the dependence is not quite as strong as in the normal-gravity case (fig. 3). As with the flat-bottomed tests of reference 6, the results show a dependence on both tank and outlet size. Previous studies (refs. 5 and 6) have suggested a Weber correlation for the data. The correlating equation given in reference 6 for flat-bottomed tanks as

$$\frac{Q_o^2}{\beta R^3} = 4000 \left( \frac{h_{cr}}{R} \right)^8 \quad (5)$$

may be rearranged into the more convenient form

$$\frac{h_{cr}}{R} = 0.355 \left( \frac{Q_o^2}{\beta R^3} \right)^{0.125} \quad (6)$$

The experimental data of this study were compared with this form of the equation and are presented in figure 6. From figure 6, it is evident that except for the coefficient of the equation, the identical Weber relation used in reference 6 for the flat-bottomed tanks may be used to correlate the data for the hemispherically bottomed tanks. The coefficient of 0.355 is replaced by 0.375. The resulting equation becomes

$$\frac{h_{cr}}{R} = 0.375 \left( \frac{Q_o^2}{\beta R^3} \right)^{0.125} \quad (7)$$

This represents an increase in critical height of the order of 8 to 12 percent above the corresponding values found in reference 6. This slight increase may have been caused by the fact that to satisfy the continuity equation the moving interface has to accelerate as it enters the decreasing cross-sectional area of the hemisphere. This slightly higher velocity (at the same volumetric flow rate) results in the slightly higher critical height.

It is also possible to further rearrange the form of the Weber number as shown in figure 6 into the form  $We = \pi^2 (v_o^2 r_o / \beta) (r_o / R)^3$ . As in the normal-gravity case, it should be noted that both forms are just two different methods of presenting the same data: one containing a flow rate  $Q_o$  and the other containing a form of the Weber number based on outlet velocity  $V_o$  and radius  $r_o$  times a radius ratio cubed. If the outlet radius is considered to be the significant characteristic length, the second method may be preferred, since in this form  $r_o$  is an explicit parameter. If, however, the interface curvature is considered to be the most important controlling dimension, the first method may have more physical significance since the radius of curvature of the interface is directly related to the tank radius  $R$ .

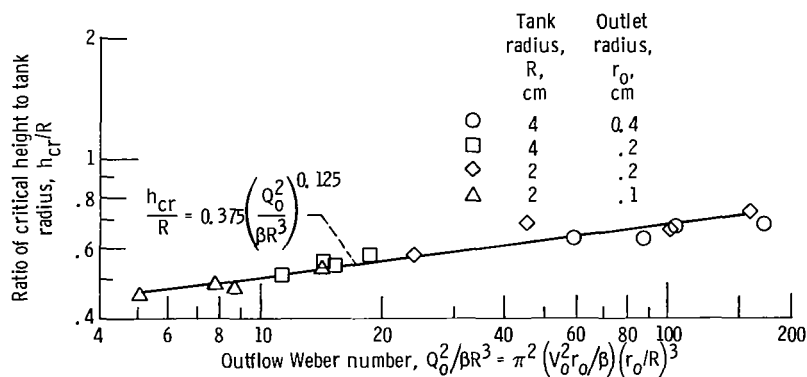


Figure 6. - Incipience of vapor ingestion in weightlessness as function of outflow Weber number.

## Liquid Residuals in Weightlessness

The liquid residual, defined as the amount of liquid remaining in a tank at the instant of vapor ingestion, is of considerable importance in determining the relative merits of various draining systems. Since the average flow rate, the total draining time up to vapor ingestion, and the initial liquid volume were known in each of the test cases, the volume remaining at vapor ingestion was calculated for each test run in weightlessness.

The results of these calculations are presented in figure 7 in nondimensional form as residual fractions. The residual fraction is the ratio of the residual liquid volume at vapor ingestion to a reference volume, which in this work is taken as the volume of the hemispherical tank bottom. The residual fractions are shown as functions of the correlating Weber number. The figure includes data for both 2- and 3-tank-radii initial filling levels.

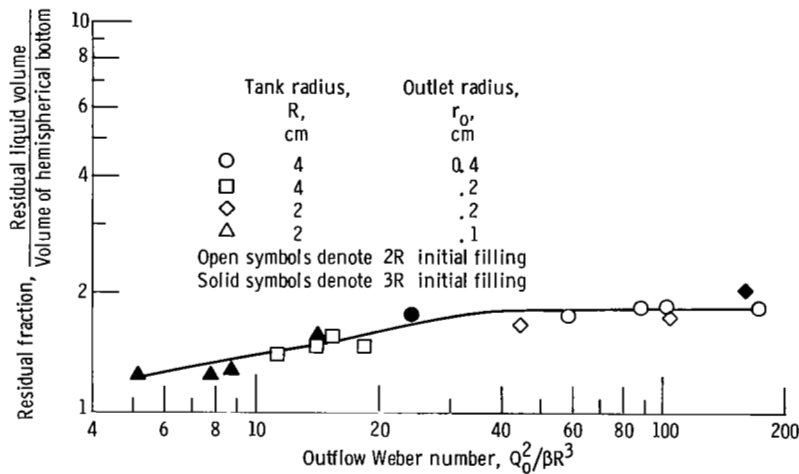


Figure 7. - Liquid residuals in weightlessness.

Note that the residual fraction increases with increasing Weber number up to a point ( $We \approx 40$ ), and then remains relatively constant. This trend is consistent with previous observations (refs. 1 and 2), where it was shown that as the outflow rate (or  $We$ ) was increased, the interface became more distorted. In the referenced works this behavior was observed up to a limiting Weber number, after which the distortion became a constant. The higher interface distortions cause more liquid to "hang up" on the tank wall, which, in turn, is reflected in the higher residuals. As the distortion levels off, so does the residual fraction. It is interesting to note that the data appear

to be almost completely normalized by the use of the reference volume in the denominator of the residual fraction for both the 2R and 3R initial filling cases. The greater initial volume in the 3R case did not result in a large increase in residual volume. Since data were obtained at only two discrete initial filling levels, however, no complete parametric spread with tank radius may be predicted. A large spread is not expected because the higher initial filling adds only a small increment to the residual, as a result of the thinning liquid layer on the wall farther from the interface low point. For these reasons only one correlating line is presented in figure 7 in spite of the possibility of a slight parametric spread with the initial filling level.

## SUMMARY OF RESULTS

A study of the vapor ingestion phenomenon in hemispherically bottomed cylindrical tanks has been conducted in normal gravity and in a weightless environment. Data were obtained for 2- and 4-centimeter-radius tank sizes, four outlet sizes, ethanol as the test fluid, and a range of flow rates. The results are summarized as follows:

1. The vapor ingestion height in normal gravity, defined as the liquid-vapor-interface height away from the drain at the time of vapor ingestion, was scaled by a Froude number similar to that used in reference 6 but modified to include a geometric term  $(R/r_o)^2$ . The equation

$$\frac{h_{vi}}{r_o} = 1.03 \left[ \left( \frac{R}{r_o} \right)^2 \left( \frac{V_o^2}{2g_o r_o} \right) \right]^{0.143}$$

was found to correlate the results for the range tested, where  $h_{vi}$  is the vapor ingestion height,  $r_o$  is the outlet radius,  $R$  is the tank radius,  $V_o$  is the average outflow velocity, and  $g_o$  is acceleration due to gravity.

2. In weightlessness, the critical height, defined as the liquid-vapor interface height above the drain at the incipience of vapor ingestion may be scaled by a Weber relation,

$$\frac{h_{cr}}{R} = 0.375 \left( \frac{Q_o^2}{\beta R^3} \right)^{0.125}$$

where  $h_{cr}$  is the critical height (height of liquid-vapor interface at incipience of vapor ingestion),  $Q_o$  is the outflow rate, and  $\beta$  is the specific surface tension. This equation is identical to that of reference 6 with the exception of the coefficient, which in that case was 0.355, and reflects the observation that the critical heights  $h_{cr}$  for the hemispherically bottomed tanks were always higher than those reported for the flat-bottomed tanks at the same Weber number. The fraction of liquid remaining in the tank at the time of vapor ingestion increases up to a Weber number  $Q_o^2/\beta R^3$  of approximately 40, after which it remains essentially constant.

Lewis Research Center,  
National Aeronautics and Space Administration  
Cleveland, Ohio, November 21, 1969,  
124-08.

## APPENDIX - APPARATUS AND PROCEDURE

### Test Facility

The experimental data for this study were obtained in the Lewis Research Center's 2.2-Second Zero-Gravity Facility. A schematic drawing of this facility is shown in figure 8. The facility consists of a building 6.4 meters (21 ft) square by 30.5 meters (100 ft) tall. Contained within the building is a drop area 27 meters (89 ft) long with a cross section 1.5 by 2.75 meters (5 by 9 ft).

The service building has, as its major elements, a shop and service area, a calibration room, and a controlled environment room. Those components of the experiment which require special handling are prepared in the controlled environment room. This air-conditioned and filtered room (shown in fig. 9) contains an ultrasonic cleaning system and the laboratory equipment necessary for handling test liquids.

Mode of operation. - A 2.2-second period of weightlessness is obtained by allowing the experiment package to free fall from the top of the drop area. In order to minimize drag on the experiment package, it is enclosed in a drag shield, designed with a high ratio of weight to frontal area and a low drag coefficient. The relative motion of the experiment package with respect to the drag shield during a test is shown in figure 10. Throughout the test the experiment package and drag shield fall freely and independently of each other; that is, no guide wires, electrical lines, etc., are connected to either. Therefore, the only force acting on the freely falling experiment package is the air drag associated with the relative motion of the package within the enclosure of the drag shield. This air drag results in an equivalent gravitational acceleration acting on the experiment, which is estimated to be below  $10^{-5}$  g's.

Release system. - The experiment package, installed within the drag shield, is suspended at the top of the drop area by means of a highly stressed music wire attached to the release system. This release system consists of a double-acting air cylinder with a hard-steel knife-edge attached to the piston. Pressurization of the air cylinder drives the knife-edge against the wire, which is backed by an anvil. The resulting notch causes the wire to fail, smoothly releasing the experiment. No measurable disturbances are imparted to the package by this release procedure.

Recovery system. - After the experiment package and drag shield have traversed the total length of the drop area, they are recovered by decelerating in a 2.2-meter- (7-ft-) deep container filled with sand. The deceleration rate (averaging 15 g's) is controlled by selectively varying the tips of the deceleration spikes mounted on the bottom of the drag shield (fig. 10). At the time of impact of the drag shield in the decelerator container, the experiment package has traversed the vertical distance within the drag shield (compare figs. 10(a) and (c)).

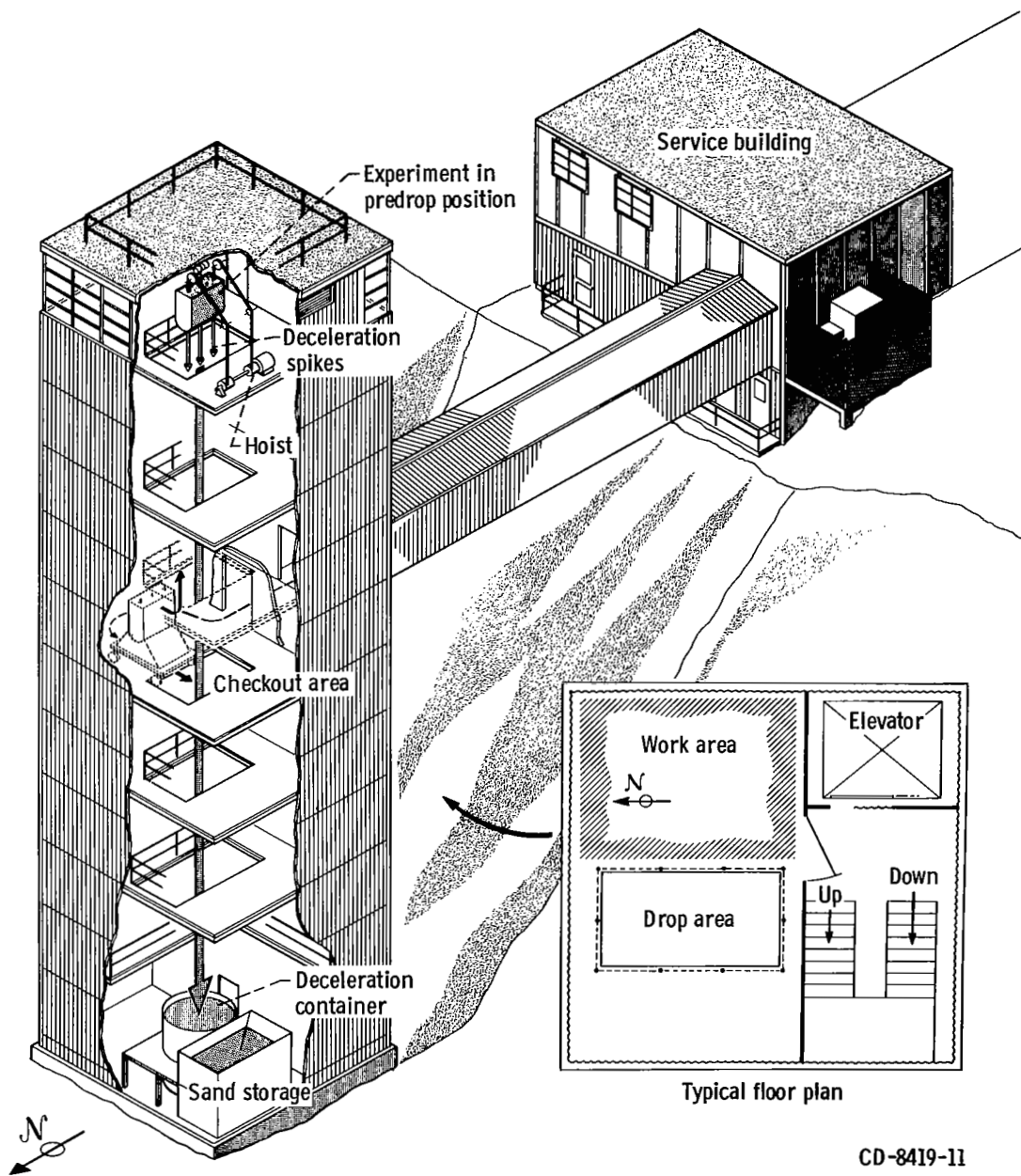
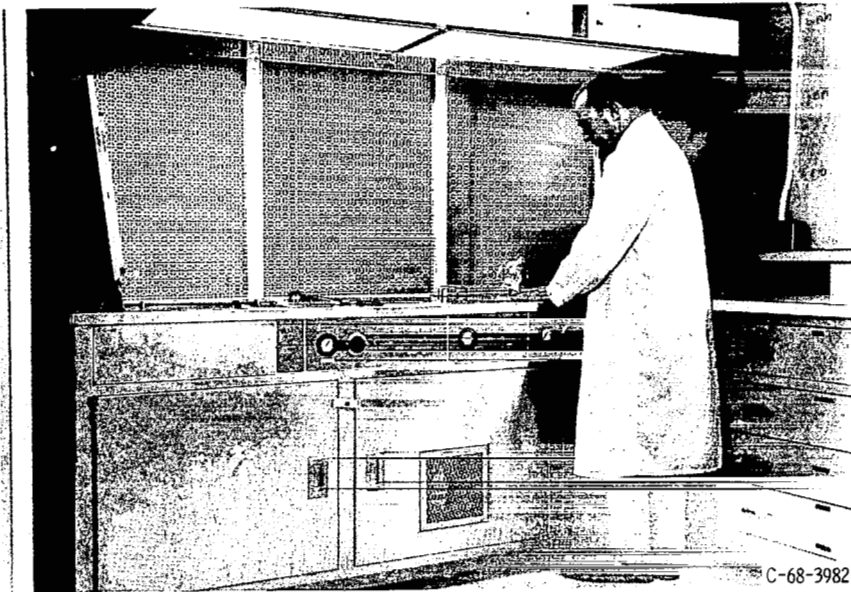
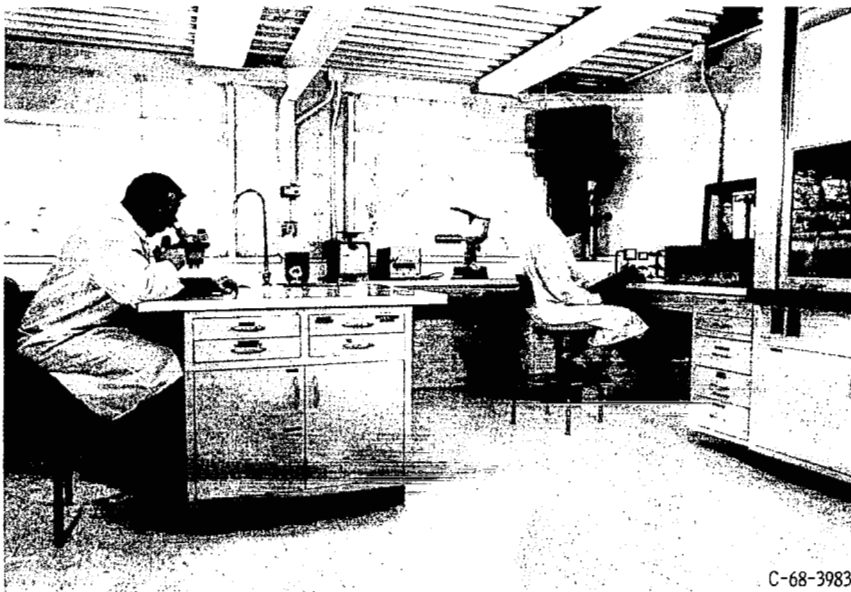


Figure 8. - 2.2-Second Zero-Gravity Facility.



C-68-3982

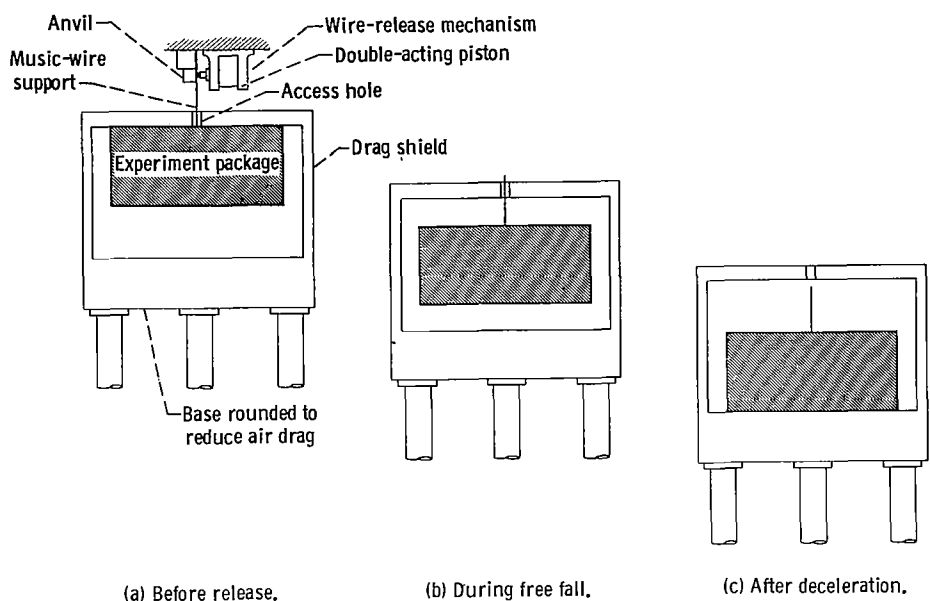
(a) Ultrasonic cleaning system.



C-68-3983

(b) Laboratory equipment.

Figure 9. - Controlled environment room.



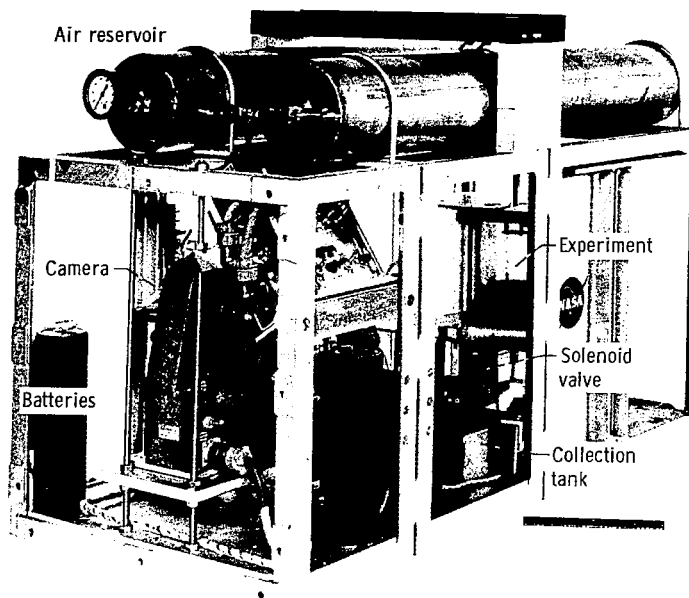
CD-7380-13

Figure 10. - Position of experiment package and drag shield before, during, and after test drop.

## Experiment Package and Test Containers

Experiment package. - The experiment package used to obtain the data for this study is shown in figure 11. It consisted of an aluminum frame in which were mounted the experiment tank and pumping system, a 16-millimeter high-speed motion picture camera, a background lighting scheme, and auxiliary equipment. The auxiliary equipment included batteries, a sequence timer, and a digital clock with divisions of 0.01 second. The pumping system is shown in schematic form in figure 12.

Test containers. - Two cylindrical tanks, 2 and 4 centimeters in radius, were used. The tanks, as shown in figure 13, consisted of plastic cylindrical sections, an inlet plate, and selected outlet hemispheres. The cylinders and hemispheres were machined from cast acrylic rod and polished until clear. The length-to-diameter ratio for the tanks ranged from 1.5 to 4 to allow for testing at various initial liquid heights. In using these tanks, strict geometric similarity was not maintained when the smaller tanks were compared to the larger ones at low initial liquid heights ( $2R$ ). The distance from the liquid-vapor interface to the pressurant inlet baffle was allowed to vary with initial liquid height. It was felt that since the vapor ingestion phenomenon under investigation was occurring very near to the outlet side of the tanks, the scaling of the vapor space above the liquid had no marked effect on the results. End plates of stainless steel incorporated O-ring seals. The inlet of each tank was baffled with a stainless-steel disk, 1 tank ra-



C-66-4639

Figure 11. - Vapor ingestion experiment package.

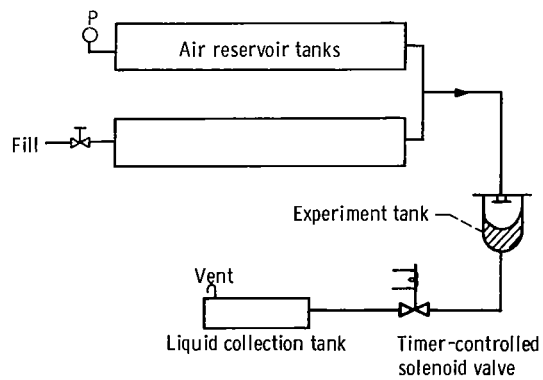
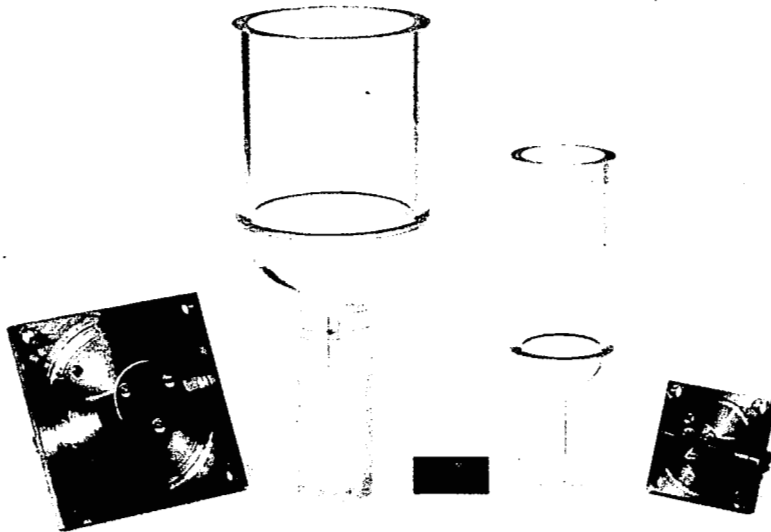


Figure 12. - Schematic drawing of pumping system.



C-69-382

Figure 13. - Test tanks.

dius in diameter, positioned  $1/2$  tank radius from the face of the inlet (fig. 13). This baffle was used to eliminate direct impingement of the pressurant on the liquid surface. The tank outlets were 0.1, 0.2, 0.4, and 0.8 centimeter in radius, and each had an outlet length at least 10 times its radius.

## Test Procedure

Experiment preparation. - Prior to a test run, the experiment tank parts were cleaned ultrasonically in warm distilled water and detergent, rinsed in distilled water, and dried in a warm-air dryer. The parts were then assembled and installed in the experiment package. The tank was filled with liquid to the desired level and checked for leakage. Draining was accomplished by means of a pressurization technique, using the air reservoir shown schematically in figure 12. This reservoir was charged to a certain pressure. The tank was drained of liquid during both normal-gravity and weightless tests by opening the solenoid valve located downstream of the tank outlet. The volume of air in the reservoir was sufficiently large in comparison with the volume of displaced liquid in the experiment tank that the change in pressure in the experiment tank was negligible during testing.

During normal-gravity testing, draining was initiated at the beginning of the test, and the motion of the liquid-vapor interface was recorded with the high-speed camera. From the resulting film sequence, the interface height as a function of draining time was

obtained. For each weightless test, on the other hand, the experiment package was allowed to free fall initially. Sufficient time was allowed for the zero-gravity interface to form. Since the time required for the interface to come to static equilibrium was too long to permit a draining test to follow, initiation of outflow was timed when the interface centerline reached its low point in its first pass through equilibrium. This time was calculated from the empirical equation

$$t = 0.62 \frac{\left(\frac{R^3}{\beta}\right)^{1/2}}{1 + 2\left(\frac{\mu^2}{\rho\sigma R}\right)^{1/4}}$$

The interface centerline velocity at this time is zero. Draining was then initiated as in normal gravity. The assumption was made that, for a particular calibrated pressure setting in the air reservoir, the resulting outflow rate in the drain was the same in weightlessness as for the normal-gravity test. This assumption has been previously verified in other tests by the authors (refs. 2 and 6).

Procedure for test drop. - Electrical timers on the experiment package are set to control the initiation and duration of all functions programmed during the drop. The experiment package is then balanced and positioned within the prebalanced drag shield. The wire support is attached to the experiment package through an access hole in the shield (see fig. 10). Properly sized spike tips are installed on the drag shield. Then the drag shield, with the experiment package inside, is hoisted to the predrop position at the top of the facility (fig. 8) and connected to an external electrical power source. The wire support is attached to the release system, and the entire assembly is suspended from the wire. After final electrical checks and switching to internal power, the system is released. After completion of the test, the experiment package and drag shield are returned to the preparation area.

Data reduction. - The photographic data obtained in these experiments were corrected for optical refraction caused by the curved plastic surface of the test tanks. A computer program was used to make these corrections, utilizing the known dimensions of the tank, the optical properties of the tank and the test fluid, and the characteristics of the photographic equipment.

## REFERENCES

1. Derdul, Joseph D.; Grubb, Lynn S.; and Petrash, Donald A.: Experimental Investigation of Liquid Outflow from Cylindrical Tanks During Weightlessness. NASA TN D-3746, 1966.
2. Berenyi, Steven G.; and Abdalla, Kaleel L.: The Liquid-Vapor Interface During Outflow in Weightlessness. NASA TM X-1811, 1969.
3. Gluck, D. F.; Gille, J. P.; Simkin, D. J.; and Zukoski, E. E.: Distortion of the Liquid Surface During Tank Discharge Under Low-G Conditions. Chem. Eng. Progr. Symp. Ser., vol. 62, no. 61, 1966, pp. 150-157.
4. Lubin, Barry T.; and Hurwitz, Matthew: Vapor Pull-Through at a Tank Drain With and Without Dielectrophoretic Baffling. Proceedings of the Conference on Long-Term Cryo-Propellant Storage in Space, NASA Marshall Space Flight Center, Huntsville, Ala., Oct. 1966, pp. 173-180.
5. Anon.: Orbital Refueling and Checkout Study. Vol. 3: Evaluation of Fluid Transfer Modes, Part 2. Rep. TI-51-67-21, vol. 3, Lockheed Missiles and Space Co. (NASA CR-93237), Feb. 12, 1968.
6. Abdalla, Kaleel L.; and Berenyi, Steven G.: Vapor Ingestion Phenomenon in Weightlessness. NASA TN D-5210, 1969.